



Analysis of non-localized creep induced strains and stresses in notches

J.E. Nuñez, G. Glinka *

Department of Mechanical Engineering, University of Waterloo, Waterloo, Ont., Canada N2L3G1

Received 23 December 2002; received in revised form 3 June 2003; accepted 11 June 2003

Abstract

A method for the estimation of time-dependent strains and stresses induced in notches has been developed. The aim of the method is to generate a solution for the creep strain and stress at the notch root based on the linear-elastic stress state, the constitutive law, and the material creep model. The proposed solution is an extension of Neuber's total strain energy density rule for the case of time-independent deformation. The method was derived for both localized and non-localized creep in a notched body. Predictions were compared with finite element data and good agreement was obtained for various geometrical and material configurations in plane stress conditions.

© 2003 Published by Elsevier Ltd.

Keywords: Notches; Non-localized creep; Plane stress; Stress–strain analysis

1. Introduction

As machines and engineering structures become more efficient, they require that their components have more complex geometries with various discontinuities such as holes, grooves, and notches. It is well known that these geometrical discontinuities induce a localized high stress concentration zone where stresses may exceed the yield limit of the material. Mechanical components work often in very demanding conditions such as a combination of high cyclic stresses with a high operating temperature. In the case of time- and temperature-dependent deformations (creep) the durability analysis requires detailed knowledge of strains and stresses in the stress concentration zone.

An accurate estimation of these local time-dependent stresses and strains can be generated by using a finite element method analysis, however the visco-plastic finite element programs are expensive, and such analyses are time consuming, particularly when simulating lengthy cyclic loading histories. Therefore, alternative more efficient methods are required to perform an estimation of stresses and strains at the notch root without compromising the accuracy.

* Corresponding author. Tel.: +1-519-888-4567; fax: +1-519-888-6197.

E-mail address: ggreg@konec.uwaterloo.ca (G. Glinka).

Nomenclature

A	Norton's power law coefficient
C_p	plastic zone correction factor
E	Young's modulus
K_t	theoretical stress concentration factor
K_ε	actual strain concentration factor
K_σ	actual stress concentration factor
K_Ω	total strain energy density concentration factor
r_p	plastic zone size
Δr_p	plastic zone size increment
t	time
Δt_n	n th time increment
α	stress exponent for creep power law
β	time exponent for creep power law
ε_{22}^0	total strain component from elastic–plastic solution
ε_{22}^{ct}	time-dependent creep strain component at the notch tip
ε_{22}^e	elastic strain at the notch tip from linear elastic solution
ε_{22}^{et}	time-dependent elastic strain component at the notch tip
ε_{22}^f	elastic strain component in a far field point
ε_{22}^{p0}	mechanically induced plastic strain at $t = 0.0$
σ_{22}^0	total stress from elastic–plastic solution
σ_{22}^e	elastic stress at the notch tip from linear elastic solution
σ_{22}^f	elastic stress component in a far field point
σ_{22}^t	time-dependent stress component
Ω^c	total strain energy density at the notch tip from linear-elastic analysis
Ω^f	total strain energy density in a far field point

To date, only a few authors have tried to develop alternative solutions for localized time-dependent creep–plasticity problems. In 1978, Chaudonneret [1] suggested that Neuber's rule [2] could be expressed in its differential form as long as the applied stress increases monotonically and is a continuous function of time. Chaudonneret and Culie [3] demonstrated that the differential form of Neuber's rule could be successfully used to predict notch root stresses and strains in creeping bodies under static and cyclic loading. However a very complex integration procedure had to be incorporated to solve the proposed differential equation, especially when creep strain was present in the net section of the specimen.

In 1984, Kurath [4] utilized a modified form of Neuber's rule to simulate the notch root stress–strain time-dependent behaviour in components made of titanium alloy, and acceptable fatigue life predictions were obtained in comparison with experimental data. Kubo and Ohji [5] extended their “small scale creep” concept, originally proposed for cracks under elastic–creep conditions, to notches under plane strain and axisymmetric bodies. The results obtained using the method by Kubo and Ohji are limited to cases where the creep is strictly localized and does not consider the effect of creep away from the notch tip.

More recently, Moftakhar et al. [6] proposed an extension of Neuber's rule [2] to estimate creep induced multiaxial strains and stresses at the notch tip. Their approach was developed assuming that the total strain energy density at the notch tip does not change when going from a linear elastic solution to a

time-dependent elastic–plastic–creep solution. Nevertheless, this assumption may be valid only for cases where the deformation is strictly localized around the point of stress concentration. In 1998, Harkegard and Sorbo [7] reformulated Chaudonneret’s model to predict creep stresses and strains in notches under constant nominal stress and constant nominal strain. The authors reduced the integration complexity of Chaudonneret’s model [1] by making extensive use of normalized forms of stress, strain and time. Good agreement was reported against generated finite element data.

The method presented below is also based on the Neuber concept but the formulation and the numerical procedure exhibit relatively high degree of time efficiency and accuracy.

2. Application of Neubers rule to creep analysis

Neuber’s rule [2] was initially proposed for elastic–plastic notched bodies in pure shear stress state. The rule is most often presented in terms relating the theoretical elastic stress concentration factor, K_t , and the actual stress and strain concentration factors,

$$K_t^2 = K_\sigma K_\epsilon. \tag{1}$$

Neuber’s rule can also be written in the form relating the hypothetical stress σ_{ij}^e and the corresponding elastic strain ϵ_{ij}^e components to the actual elastic–plastic stress σ_{ij}^0 and strain components ϵ_{ij}^0

$$\sigma_{ij}^e \epsilon_{ij}^e = \sigma_{ij}^0 \epsilon_{ij}^0. \tag{2}$$

In such a case, Eq. (1) for notched bodies in plane stress reduces to

$$\sigma_{22}^e \epsilon_{22}^e = \sigma_{22}^0 \epsilon_{22}^0. \tag{3}$$

Eq. (3) results directly from the original Neuber’s rule (1) and it can be interpreted as an equivalence of the total strain energy density.

Moftakhar et al. [6] showed that the total strain energy density at the notch tip, $\Omega = \sigma_{22}^e \epsilon_{22}^e$, remains almost constant as long as the plastic deformation remains a local event, even when stresses relax due to creep. In other words, Neuber’s rule can be directly extended to time-dependent stress and strain analysis in the following way,

$$\Omega = \sigma_{22}^e \epsilon_{22}^e = \sigma_{22}^0 \epsilon_{22}^0 = \sigma_{22}^t \epsilon_{22}^t, \tag{4}$$

where the term on the right-hand side represents the total strain energy density at a specific time, t , under constant nominal stress and constant temperature. It has been shown [8] that as long as the plastic yielding and creep remain a local event limited to the zone near the notch tip, Neuber’s rule will always overestimate the actual elastic–plastic strains and stresses. Therefore, some authors have called this the upper bound solution as opposed to the ESED method proposed by Molski and Glinka [9], which is believed to give a lower bound solution.

The graphical interpretation of the creep Neuber rule is illustrated in Fig. 1. The equivalence of the total strain energy density means that the total strain energy density obtained from a linear-elastic solution and represented by area $OB^cC^cA^c$ is equal to the area $OB^aC^aA^a$ representing the actual total strain energy density at the notch tip.

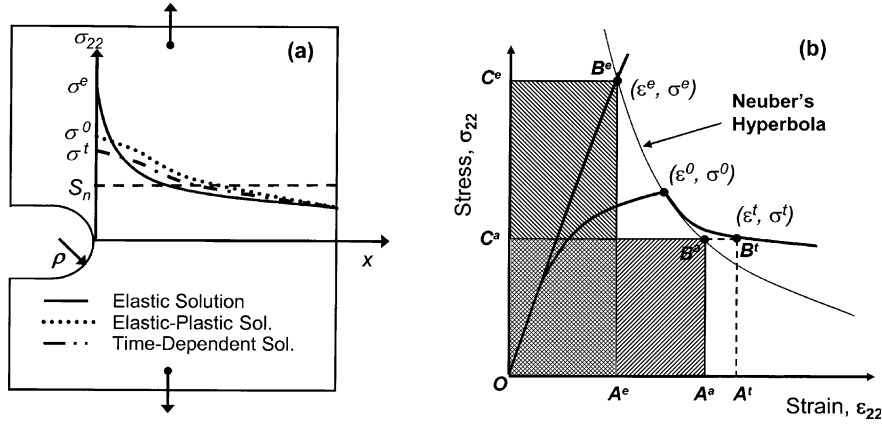


Fig. 1. (a) Stress distribution in notched specimen under tension loading. (b) Graphical interpretation of the Neuber's rule approach to creep analysis.

3. Localized creep formulation

Consider a notched body at constant temperature and subjected to constant load for an extended period of time. As long as the creep is localized it is reasonable to assume after Neuber that

$$\sigma_{22}^0 \epsilon_{22}^0 = \sigma_{22}^t \epsilon_{22}^t. \tag{5}$$

The time-dependent strain can be decomposed into its elastic ϵ_{22}^{ct} , mechanically induced plastic $\epsilon_{22}^{p(0)}$, and creep ϵ_{22}^{ct} contributions,

$$\epsilon_{22}^t = \epsilon_{22}^{ct} + \epsilon_{22}^{p0} + \epsilon_{22}^{ct}. \tag{6}$$

The mechanically induced plastic strain, ϵ_{22}^{p0} , is considered to be constant during the hold time period, since it represents the non-recoverable plastic deformation at time $t = 0.0$. This assumption suggests that during the hold time there is only a trade off between the elastic unloading and creep deformation. Substituting Eq. (6) into Eq. (5) results in

$$\sigma_{22}^0 \epsilon_{22}^0 = \sigma_{22}^t \epsilon_{22}^{ct} + \sigma_{22}^t \epsilon_{22}^{p0} + \sigma_{22}^t \epsilon_{22}^{ct}. \tag{7}$$

Differentiating Eq. (7) with respect to time leads to the following equation:

$$0.0 = \dot{\sigma}_{22}^t \epsilon_{22}^{ct} + \sigma_{22}^t \dot{\epsilon}_{22}^{ct} + \dot{\sigma}_{22}^t \epsilon_{22}^{p0} + \sigma_{22}^t \dot{\epsilon}_{22}^{ct} + \dot{\sigma}_{22}^t \epsilon_{22}^{ct}. \tag{8}$$

For a uniaxial stress state at the notch tip, the elastic strain can always be obtained as $\epsilon_{22}^{ct} = \sigma_{22}^t / E$. The elastic strain rate, on the other hand, is defined as $\dot{\epsilon}_{22}^{ct} = \dot{\sigma}_{22}^t / E$. Therefore, Eq. (8) can be written in the following form:

$$0.0 = \frac{2}{E} \sigma_{22}^t \dot{\sigma}_{22}^t + \dot{\sigma}_{22}^t \epsilon_{22}^{p0} + \sigma_{22}^t \dot{\epsilon}_{22}^{ct} + \dot{\sigma}_{22}^t \epsilon_{22}^{ct}. \tag{9}$$

Eq. (9) is the general differential equation which together with the material creep law forms the set of two equations needed for the mathematical formulation of the problem. A closed form solution to the two equations is seldom feasible particularly when creep models take complex mathematical forms. Moftakhar et al. [6] proposed a special time integration method to generate a suitable numerical solution. It was suggested to divided the integration time period into a finite number of discrete steps, Δt_n , and then to

generate solutions for subsequent time steps. Based on the proposed approach, the time derivatives can be written in the incremental form as

$$\dot{\sigma}_{22}^t = \frac{d\sigma_{22}^t}{dt} \cong \frac{\Delta\sigma_{22}^{t_n}}{\Delta t_n} = \frac{\sigma_{22}^{t_n} - \sigma_{22}^{t_{n-1}}}{t_n - t_{n-1}} \quad (10)$$

and

$$\dot{\varepsilon}_{22}^{ct} = \frac{d\varepsilon_{22}^{ct}}{dt} \cong \frac{\Delta\varepsilon_{22}^{c_n}}{\Delta t_n} = \frac{\varepsilon_{22}^{c_n} - \varepsilon_{22}^{c_{n-1}}}{t_n - t_{n-1}}. \quad (11)$$

The substitution of Eqs. (10) and (11) into Eq. (9) results in

$$0.0 = \frac{2}{E} \frac{\Delta\sigma_{22}^{t_n}}{\Delta t_n} \sigma_{22}^{t_{n-1}} + \frac{\Delta\sigma_{22}^{t_n}}{\Delta t_n} \varepsilon_{22}^{p0} + \frac{\Delta\sigma_{22}^{t_n}}{\Delta t_n} \varepsilon_{22}^{c_n} + \sigma_{22}^{t_{n-1}} \frac{\Delta\varepsilon_{22}^{c_n}}{\Delta t_n}. \quad (12)$$

The incremental equation (12) can be solved for the stress increment, $\Delta\sigma_{22}^{t_n}$, occurring during the time step, Δt_n .

$$\Delta\sigma_{22}^{t_n} = \frac{-\sigma_{22}^{t_{n-1}} \Delta\varepsilon_{22}^{c_n}}{\frac{2}{E} \sigma_{22}^{t_{n-1}} + \varepsilon_{22}^{p0} + \varepsilon_{22}^{c_n}}. \quad (13)$$

As expected, the stress increment $\Delta\sigma_{22}^{t_n}$ is negative; hence, it represents the decrement of stress relaxation at the notch tip induced by creep. The increment of creep strain, $\Delta\varepsilon_{22}^{c_n}$, can be directly obtained from the creep law $\dot{\varepsilon}_{22}^c = f(\sigma)g(t)$, which is often written in the power law form proposed by Norton [10]:

$$\dot{\varepsilon}_{22}^c(\sigma; t) = A\sigma^\alpha t^\beta, \quad (14)$$

where A , α and β are material constants for a given temperature. The incremental form of the creep law used in the model is subsequently written as

$$\Delta\varepsilon_{22}^{c_n} = \Delta t_n \cdot \dot{\varepsilon}_{22}^c(\sigma; t). \quad (15)$$

4. Non-localized creep formulation

In most real-life components working in creep conditions, the creep strains in the far field albeit relatively low might be important as well. Analogously to the notch tip, the material in the rest of the component may creep as well. As the stress at the notch tip relaxes, so does the constraint provided by the material from the far field region. Therefore, with the constraint being relaxed, additional creep deformation at the notch tip is allowed for. This situation is the so-called *non-localized*, or *gross creep* conditions.

Extending further the idea of the equivalence of the total strain energy density, an extra amount of energy is needed to account for the constraint loss imposed on the notch tip by the far field. Moftakhar et al. [8] suggested that the total strain energy density changes occurring in the far field, Ω^{fc} , produce similar but magnified effects at the notch tip. A good measure of such a magnification is the so-called *total strain energy density concentration factor*, K_Ω .

The strain energy concentration factor proposed by Moftakhar et al. [6] is defined as

$$K_\Omega = \frac{\Omega^e}{\Omega^f} = \frac{\sigma_{22}^e \varepsilon_{22}^e}{\sigma_{22}^f \varepsilon_{22}^f}, \quad (16)$$

where Ω^e is the total strain energy density at the notch tip obtained from a linear elastic analysis, and Ω^f is the total strain energy density at a pre-defined point in the far field also obtained from the linear elastic solution.

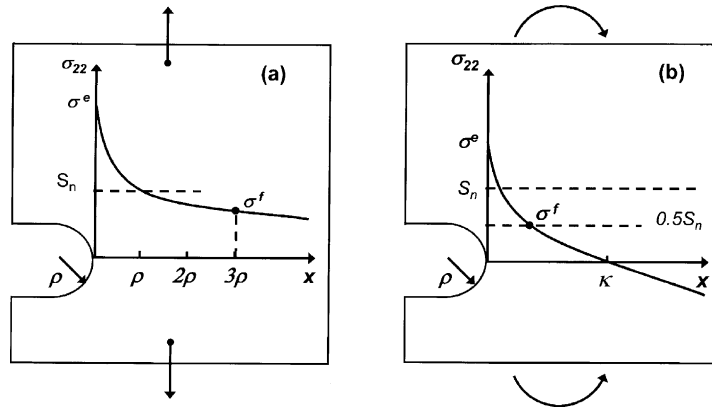


Fig. 2. Graphical representation of the far field stress definition in a notched component: (a) uniaxial tension, (b) pure bending.

The definition of *far field* used in our analysis is shown in Fig. 2. The far field stress in the case of a body subjected to pure axial load is assumed to be equal to the elastic stress found at a distance of three times the notch radius. In the case of pure bending load, the far field stress is defined as one-half of the nominal simple bending stress.

The effect the creep in the far field under constant load has on the notch tip behaviour can be interpreted as an additional input of strain energy density. This additional increment of strain energy density must be included into Eq. (5),

$$\sigma_{22}^0 \varepsilon_{22}^0 + K_{\Omega} \Omega^{cf} = \sigma_{22}^t \varepsilon_{22}^t, \tag{17}$$

where

$$\Omega^{cf} = \sigma_{22}^f \varepsilon_{22}^{cf}. \tag{18}$$

Expression (18) represents the total strain energy density contributed as a result of the local and the far field creep. Decomposing the time-dependent strain into its elastic, initial plastic and creep, the strain energy density equation at the notch tip can be written as

$$\sigma_{22}^0 \varepsilon_{22}^0 + K_{\Omega} \sigma_{22}^f \varepsilon_{22}^{cf} = \sigma_{22}^t \varepsilon_{22}^{et} + \sigma_{22}^t \varepsilon_{22}^{p0} + \sigma_{22}^t \varepsilon_{22}^{ct}. \tag{19}$$

Differentiating Eq. (19) with respect to time, results in Eq. (20).

$$K_{\Omega} (\dot{\sigma}_{22}^f \varepsilon_{22}^{cf} + \sigma_{22}^f \dot{\varepsilon}_{22}^{cf}) = \dot{\sigma}_{22}^t \varepsilon_{22}^{et} + \sigma_{22}^t \dot{\varepsilon}_{22}^{et} + \dot{\sigma}_{22}^t \varepsilon_{22}^{p0} + \sigma_{22}^t \dot{\varepsilon}_{22}^{ct} + \dot{\sigma}_{22}^t \varepsilon_{22}^{ct}. \tag{20}$$

It was observed that the far field stress changes due to creep are relatively small compared to the stress changes at the notch tip or none if the external load is constant. Therefore the strain energy density changes in the far field are mainly due to the change in strain. As a result, it can be assumed that the far field stress σ_{22}^f remains constant during the hold time, and it takes the value of the elastic stress in the far field calculated at time $t = 0.0$. This assumption is drawn from the fact that under constant load the stress due to equilibrium must balance out the load and therefore the far stress field cannot drastically change.

$$\sigma_{22}^f = \sigma_{22}^f|_{t=0.0} = \sigma_{22}^{f0}. \tag{21}$$

Furthermore, the elastic strains can be replaced according to the Hooke law by stress. After subsequent substitutions Eq. (20) can be reduced to

$$K_{\Omega} \sigma_{22}^{f0} \dot{\epsilon}_{22}^{cf} = \frac{2}{E} \sigma_{22}^t \dot{\sigma}_{22}^t + \dot{\sigma}_{22}^t \epsilon_{22}^{p0} + \sigma_{22}^t \dot{\epsilon}_{22}^{ct} + \dot{\sigma}_{22}^t \epsilon_{22}^{ct}. \quad (22)$$

In order to obtain the recursive form of the general differential equation, Eqs. (10) and (11) need to be substituted into Eq. (22).

$$K_{\Omega} \sigma_{22}^{f0} \frac{\Delta \epsilon_{22}^{cf_n}}{\Delta t_n} = \frac{2}{E} \frac{\Delta \sigma_{22}^{t_n}}{\Delta t_n} \sigma_{22}^{t_{n-1}} + \frac{\Delta \sigma_{22}^{t_n}}{\Delta t_n} \epsilon_{22}^{p0} + \frac{\Delta \sigma_{22}^{t_n}}{\Delta t_n} \epsilon_{22}^{c_n} + \sigma_{22}^{t_{n-1}} \frac{\Delta \epsilon_{22}^{c_n}}{\Delta t_n}. \quad (23)$$

Solving for the actual stress increment, $\Delta \sigma_{22}^{t_n}$, at the notch tip, the following expression is obtained:

$$\Delta \sigma_{22}^{t_n} = \frac{K_{\Omega} \sigma_{22}^{f0} \Delta \epsilon_{22}^{cf_n} - \sigma_{22}^{t_{n-1}} \Delta \epsilon_{22}^{c_n}}{\frac{2}{E} \sigma_{22}^{t_{n-1}} + \epsilon_{22}^{p0} + \epsilon_{22}^{c_n}}, \quad (24)$$

where

$$|K_{\Omega} \sigma_{22}^{f0} \Delta \epsilon_{22}^{cf_n}| < |\sigma_{22}^{t_{n-1}} \Delta \epsilon_{22}^{c_n}|. \quad (25)$$

Eq. (24) is valid as long as inequality (25) is true. Some combinations of load conditions and component geometry may cause the left-hand side term of expression (25) to be greater than the term on the right-hand side. However, such situations are seldom encountered.

5. Plastic zone adjustment

Moftakhar et al. [8] has shown that in case of the presence of gross creep plasticity, Neuber's rule approach tends to under estimate the real stresses and strains at the notch tip. In order to correct for such an effect, a correction needs to be introduced for the calculation of the initial total strain energy density obtained from the linear elastic analysis. Therefore, Glinka [11] introduced the plastic zone correction factor in order to compensate for the stress redistribution occurring in the notch tip region caused by the localized plastic yielding. This correction factor was derived analogously to Irwin's [12] plastic zone correction factor proposed for sharp notches and cracks.

Glinka's plastic zone correction factor, C_p , has been defined as,

$$C_p = 1 + \frac{\Delta r_p}{r_p}. \quad (26)$$

A complete procedure of how the plastic zone size, r_p , and the plastic zone increment, Δr_p , can be estimated for components subjected to tension and pure bending is given in Ref. [11].

Once the plastic zone correction factor is estimated, the total strain energy density equation (19) can be written as

$$\sigma_{22}^0 \epsilon_{22}^0 + (K_{\Omega} C_p) \sigma_{22}^f \epsilon_{22}^{cf} = \sigma_{22}^t \epsilon_{22}^{ct} + \sigma_{22}^t \epsilon_{22}^{p0} + \sigma_{22}^t \epsilon_{22}^{ct}. \quad (27)$$

The resulting final expression for the calculation of the stress increment at the notch tip is

$$\Delta \sigma_{22}^{t_n} = \frac{(K_{\Omega} C_p) \sigma_{22}^{f0} \Delta \epsilon_{22}^{cf_n} - \sigma_{22}^{t_{n-1}} \Delta \epsilon_{22}^{c_n}}{\frac{2}{E} \sigma_{22}^{t_{n-1}} + \epsilon_{22}^{p0} + \epsilon_{22}^{c_n}}. \quad (28)$$

And the actual strain increment can be calculated as

$$\Delta \epsilon_{22}^{t_n} = \Delta \epsilon_{22}^{c_n} - \frac{\Delta \sigma_{22}^{t_n}}{E}. \quad (29)$$

6. Validation of the proposed model

In order to assess the accuracy of the proposed model, finite element analyses of creep in notched components were carried out using the ABAQUS 6.1 [13] finite element software. The elastic–plastic stress–strain curves, shown in Fig. 3, were given in the form of a series of linear segments. The calculations from both the finite element and the proposed method were carried out using the *strain hardening* scheme (as opposed to a *time hardening* algorithm), which for a power law creep model of the form of Eq. (14) becomes the following expression [13]:

$$\dot{\varepsilon}_{\text{eq}}^c = (A(\sigma_{\text{eq}})^\alpha [(\beta + 1)\varepsilon_{\text{eq}}^c]^\beta)^{1/\beta+1}, \quad (30)$$

where $\varepsilon_{\text{eq}}^c$ is the uniaxial equivalent creep strain, and σ_{eq} is the uniaxial equivalent deviatoric stress. The particular form of the flow rule used in the analyses can be expressed as

$$\dot{\varepsilon}_{ij}^c = \dot{\varepsilon}_{\text{eq}}^c \cdot n_{ij}, \quad (31)$$

where n_{ij} represents the gradient of the deviatoric stress potential.

Four different cases were analyzed including various geometrical, load, and material properties data; two of them (*case C* and *case D*) accounted for the primary creep as well by introducing a value for parameter β different than zero. Elements at the notch tip had an average size of 1/10 of the notch radius in order to account for the high strain gradient near the notch tip. The mesh used for *case D* can be observed in Fig. 4. All components were subjected to a constant external load held for a pre-defined period of time (see Figs. 5–8). The analyzed configurations were assumed to be in plane stress conditions resulting in uniaxial stress–strain state at the notch tip. Only the maximum strain component and corresponding stress were generated using the proposed method.

The loading histories applied consisted of two steps, namely: instantaneous loading from zero to maximum load, and hold time under constant maximum load. No creep was generated during the first loading period; however, significant amount of mechanically induced plastic strain was generated by the load excursion from zero to max (see Figs. 5–8). The Neuber-type analysis of creep commenced from the

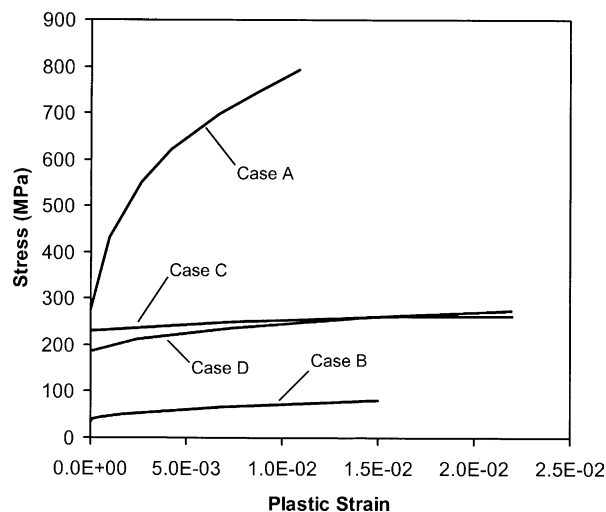


Fig. 3. Mechanical elastic–plastic stress–strain curves.

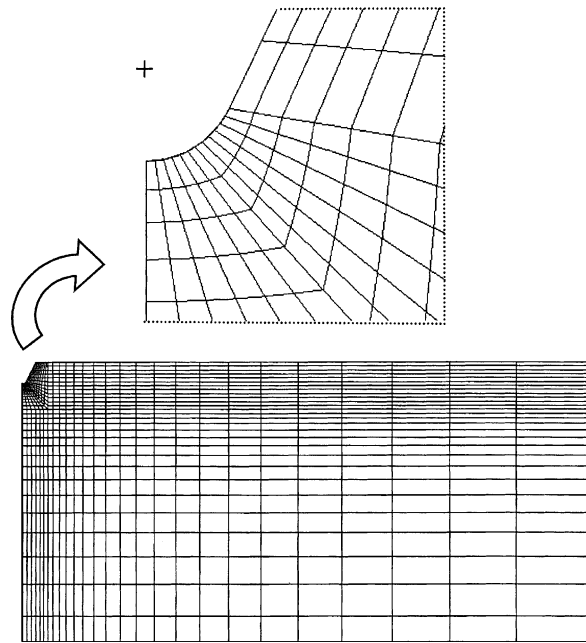


Fig. 4. Mesh used for the finite element analyses of case 'D'.

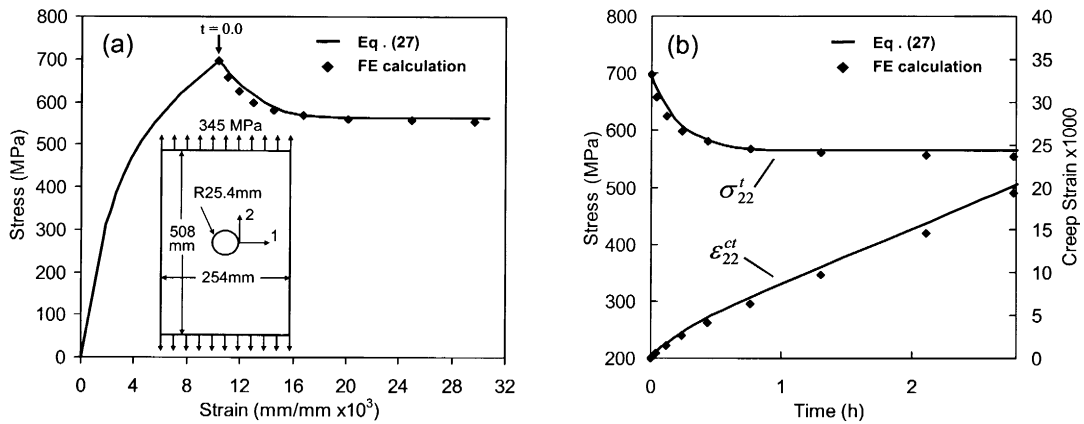


Fig. 5. Results for case 'A': (a) stress–strain response for a nominal stress of 430 MPa and a hold time of 3 h, (b) variation of stress and creep strain with time.

moment after reaching the maximum load which was also the reference point for time measurement ($t = 0.0$).

The material constants, time step size, stress concentration factors, as well as the calculated plastic zone correction factors (using Ref. [11]) for all four cases are listed in Table 1. Although, the materials properties utilized do not completely represent those of real materials, they were selected so a large enough range of yield stresses and hardening exponents would be covered. Some of the materials in which the properties are

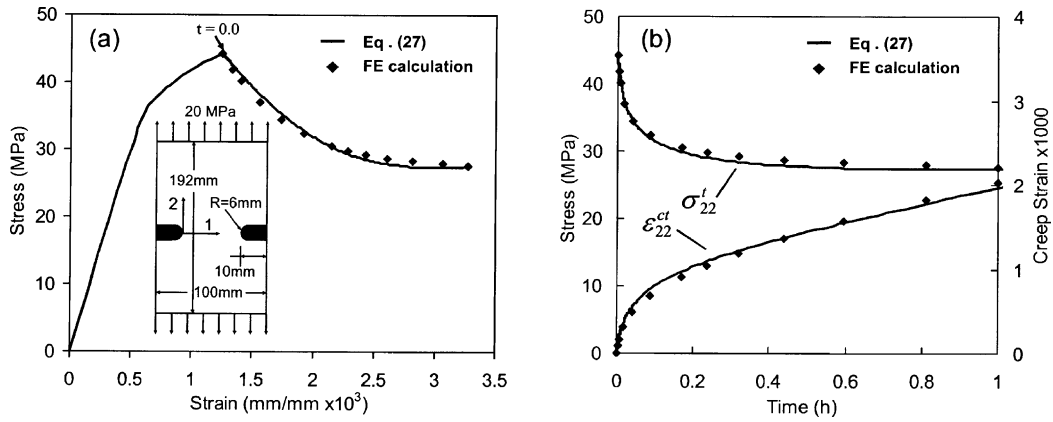


Fig. 6. Results for case ‘B’: (a) stress–strain response for a nominal stress of 25 MPa and a hold time of 1 h, (b) variation of stress and creep strain with time.

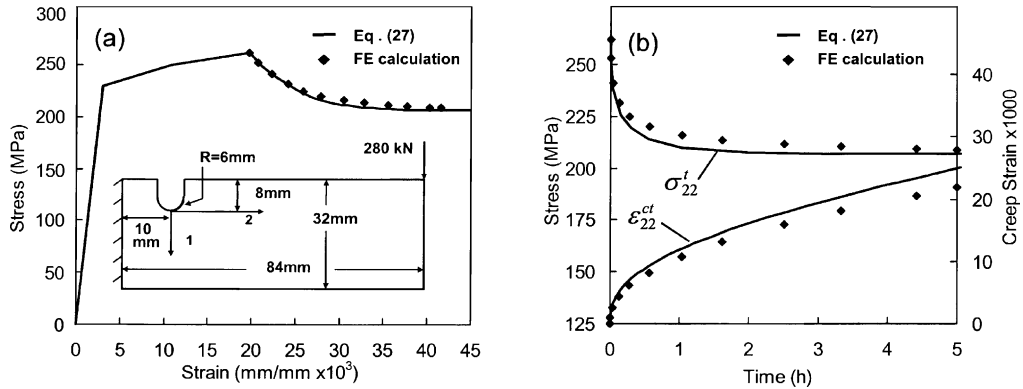


Fig. 7. Results for case ‘C’: (a) stress–strain response for a nominal stress of 191 MPa and a hold time of 5 h, (b) variation of stress and creep strain with time.

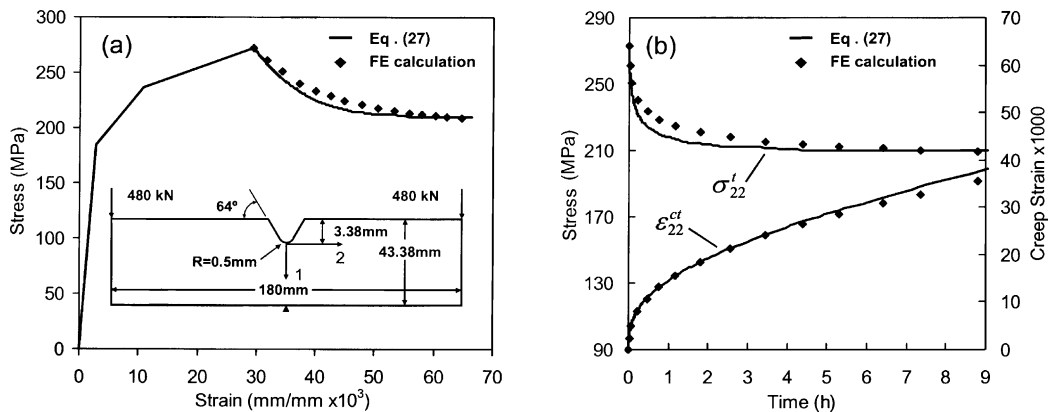


Fig. 8. Results for case ‘D’: (a) stress–strain response for a nominal stress of 157 MPa and a hold time of 9 h, (b) variation of stress and creep strain with time.

Table 1
 Constants and material properties for validation of proposed solution

	Elastic–plastic properties		Creep constants			Time increment Δt (h)	Calculated factors	
	σ_y (MPa)	E (MPa)	A (1/h)	α	β		K_t	C_p^a
Case A: plate with a circular hole	275.8	191,000	1.800×10^{-12}	5.0	0.0	1×10^{-6}	2.78	1.55
Case B: plate with edge notches	34.4	58,800	9.484×10^{-15}	7.7	0.0	1×10^{-5}	2.94	1.17
Case C: notched cantilever beam	230	75,000	6.960×10^{-14}	4.7	−0.4	1×10^{-6}	3.00	1.22
Case D: three-point bending beam	185	68,000	6.960×10^{-14}	4.7	−0.4	1×10^{-6}	5.38	1.59

^a For nominal load level investigated.

based are annealed aluminium, 316L stainless steel, and the titanium alloy Ti–6Al–4V. The geometrical configurations of the analyzed components and results obtained from both the proposed method and finite element analyses are shown in Figs. 5–8. The agreement between the finite element and the proposed method results was very good in all four cases analyzed.

6.1. Final set of equations to be solved for each increment

- Increment of creep strain (Eq. (15))

$$\Delta \epsilon_{22}^{c_n} = \Delta t_n \cdot \dot{\epsilon}_{22}^c(\sigma; t).$$

- Decrement of stress due to creep (Eq. (28))

$$\Delta \sigma_{22}^{t_n} = \frac{(K_\Omega C_p) \sigma_{22}^{f0} \Delta \epsilon_{22}^{c_{f_n}} - \sigma_{22}^{t_{n-1}} \Delta \epsilon_{22}^{c_n}}{\frac{2}{E} \sigma_{22}^{t_{n-1}} + \epsilon^{p0} + \epsilon_{22}^{c_n}}.$$

- Increment of total strain (Eq. (29))

$$\Delta \epsilon_{22}^{t_n} = \Delta \epsilon_{22}^{c_n} - \frac{\Delta \sigma_{22}^{t_n}}{E}.$$

6.2. General stepwise procedure to generate a solution

1. Determine the notch tip stress, σ_{22}^e , and strain, ϵ_{22}^e , using the linear-elastic analysis.
2. Determine the elastic–plastic stress, σ_{22}^0 , and strain, ϵ_{22}^0 , using the original Neuber’s rule [2], the ESED method [9], or finite element analysis.
3. Begin the creep analysis by calculating the increment of creep strain, $\Delta \epsilon_{22}^{c_n}$, for a given time increment, Δt_n . A specific creep hardening rule has to be followed.
4. Determine the decrement of stress, $\Delta \sigma_{22}^{t_n}$, due to the previously calculated increment of creep strain, $\Delta \epsilon_{22}^{c_n}$.
5. Determine the increment of total strain in the notch tip, $\Delta \epsilon_{22}^{t_n}$, for a given time increment, Δt_n .
6. Repeat steps from 3 to 5 until the total time is completed.

The detailed algorithm for calculating the stress–strain response with time is shown in Fig. 9.

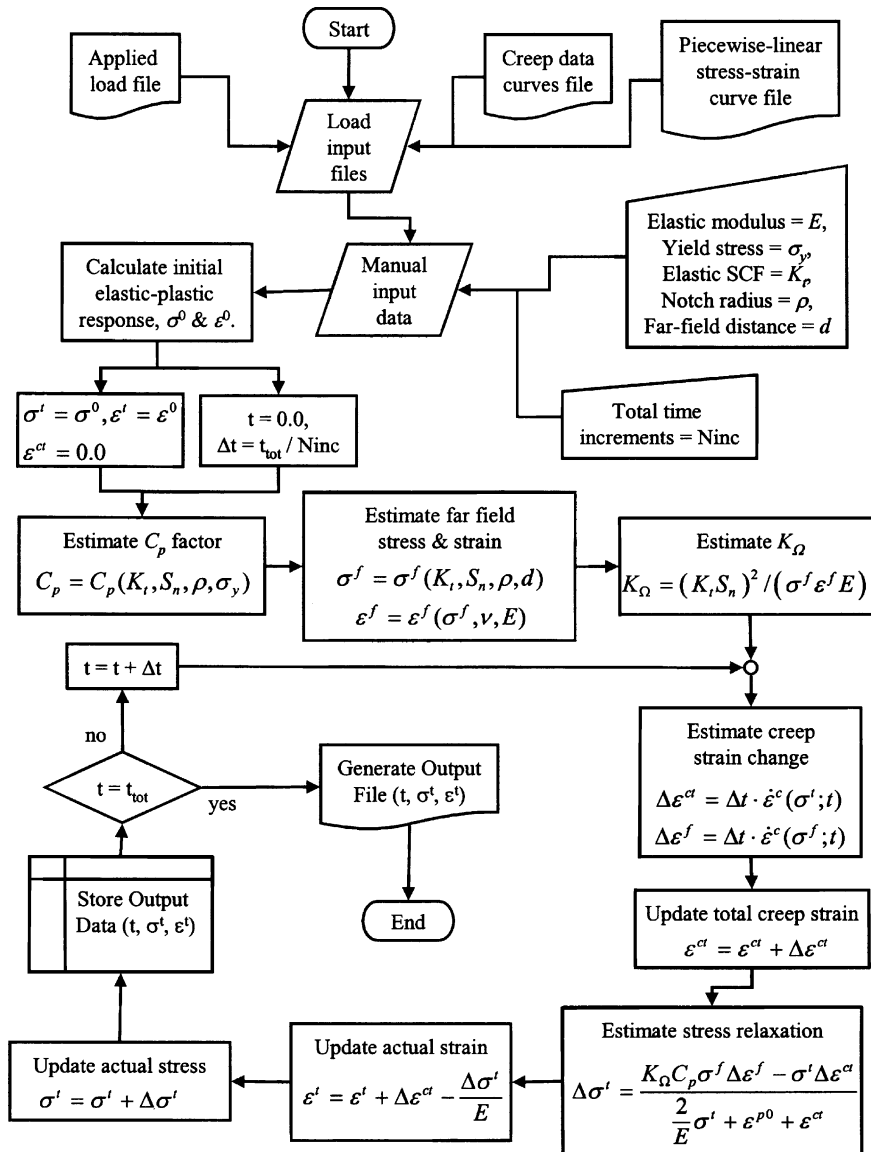


Fig. 9. General time-integration algorithm for notched components under hold-time load and non-localized creep.

7. Conclusions

The proposed solution for creep in notches makes it possible to calculate creep-induced stresses and strains for a variety of geometrical and load configurations. The comparison with the finite element data revealed that the proposed methodology predicted correctly stresses and strains even in cases where the primary creep ($\beta \neq 0.0$) had to be taken into account. The agreement between results obtained with Eqs. (28) and (29), and those obtained from the finite element analysis was within 5% on stresses and 10% on strains for the majority of the cases analyzed to date (Figs. 5–8).

The method can be easily programmed and it yields good results for various creep data and creep hardening models. It is particularly suitable for simulating creep deformation in notches under constant load. However, it is anticipated that the method can be extended for variable loading such as those in components subjected to cyclic loading.

References

- [1] Chaudonneret M. Calcul de concentrations de contrainte en elastoviscoplasticité, PhD Thesis Dissertation, Office Natl d'Etudes et de Recherches Aérospatiales (ONERA), Chatillon, France, 1978.
- [2] Neuber H. Theory of stress concentration for shear-strained prismatic bodies with arbitrary nonlinear stress-strain law. *J Appl Mech, Trans ASME* 1961;28:544–51.
- [3] Chaudonneret M, Culie JP. Adaptation of Neuber's theory to stress concentration in viscoplasticity. *Rech Aérospatiale (English Edition)* 1985;(4):33–40.
- [4] Kurath P. Extension of the local strain fatigue analysis concepts to incorporate time dependent deformation in Ti–6Al–4V at room temperature, T&AM Report no. 464. Urbana, IL, USA: The University of Illinois; 1984.
- [5] Kubo S, Ohji K. Development of simple methods for predicting plane-strain and axi-symmetric stress relaxation at notches in elastic-creep bodies. In: *Proceedings of the International Conference on Creep*. Tokyo, Japan: JSME; 1986. p. 417–22.
- [6] Moftakhar A, Glinka G, Scarth D, Kawa D. Multiaxial stress-strain creep analysis for notches. In: *ASTM Special Technical Publication 1184*. Philadelphia, PA, USA: ASTM; 1994. p. 230–43.
- [7] Harkegard G, Sorbo S. Applicability of Neuber's rule to the analysis of stress and strain concentration under creep conditions. *J Engng Mater Technol, Trans ASME* 1998;120(3):224–9.
- [8] Moftakhar A, Buczynski A, Glinka G. Calculation of elasto-plastic strains and stresses in notches under multiaxial loading. *Int J Fract* 1995;70(4):357–73.
- [9] Molski K, Glinka G. A method of elastic-plastic stress and strain calculation at a notch root. *Mater Sci Engng* 1981;50(1):93–100.
- [10] Norton FH. *Creep of Steel at High Temperatures*. New York: McGraw-Hill; 1929.
- [11] Glinka G. Calculation of inelastic notch-tip strain-stress histories under cyclic loading. *Engng Fract Mech* 1985;22(5):839–54.
- [12] Irwin GR. *Linear fracture mechanics, fracture transition and fracture control*. *Engng Fract Mech* 1968;1:241–57.
- [13] Hibbit, Karlsson & Sorensen, Inc., 2000, ABAQUS 6.1, HKS: Pawtucket, RI, USA.